海洋安全學會誌 第 3 卷 第 2 號, pp. 23~31, 1997. 7.

論 文

Dynamic Behavior of the keyhole in Laser Processing

*Jong-Do Kim**

레이저 가공에 있어서 키홀의 동적거동

김 종 도

<목 차>

Abstract

The results of high speed photography, acoustic emission detection and plasma UV radiation intensity measurement during CO2 laser welding of stainless steel 304 are presented. Video images with high spatial and temporal resolution allowed to observe the melt dynamics and keyhole evolution. The existence of a high speed melt flow which originated from the part of weld pool and flowed along the sides wall of keyhole was confirmed by the slag motion on the weld pool. the characteristic frequencies of flow instability and keyhole fluctuations at different welding speed were measured and compared with the results of Fourier analyses of temporal acoustic emission (AE) and light emission (LE) spectra. The experimental results were compared with the newly developed numerical model of keyhole dynamics. (The model is based on the assumption that the propagation of front part of keyhole into material is due to the melt ejection driven by laser induced surface evaporation.) The calculations predict that a high speed melt flow is induced at the front part of keyhole when the sample travel speed exceeds several 10 mm/s. The numerical analysis also shows the hump formation on the front keyhole wall surface. Experimentally observed melt behavior and transformation of the AE and LE spectra with variation of welding speed are qualitatively in good agreement with the model predictions.

* Joining and Welding Research Institute, Osaka University
(Applied High Temperature Engineering course)
11-1 Mihogaoka, Ibaraki, Osaka 567,Japan

1. Introduction

Vaporization recoil force during keyhole laser welding can result in melt ejection from the interaction zone only if it exceeds the counteracting forces induced by the surface tension, gravitation and melt flow around keyhole. In the majority of works it is assumed that there exist a balance between recoil force from one side and sum of surface tensional force, gravitational force and melt flow force from other side, Thus, it is indirectly assumed that the keyhole formation time is shorter than any other characteristic time, and the keyhole has reached final phase existing, practically, in the steady state except for the small amplitude shape fluctuations around the equilibrium position. If the equilibrium assumption is true, no flow generation can be produced by the recoil force and the melt motion in the weld pool can be considered as the flow around cylindrical body-keyhole.

However, it has been experimentally observed that the keyhole is not in quasistationary state but it fluctuates violently in size and shape1,2). Arata and others1) observed the humps formation at the keyhole front wall of EB and laser welding and their scraping phenomena along the front wall, which resulted in the formation of spiking. Kim and others2-4) observed the unstable keyhole behavior in pulsed laser spot welding and this instability was closely related to the formation of characteristic porosity. Also, it is widely known that spattering is likely to occur in the spot or low consideration based on the force balance, Consequently, for the typical industrially used processing conditions the force balance assumption at the keyhole wall is not satisfied, and the recoil force exceeds counteracting forces inducing melt ejection and thus driving front part of the keyhole and weld pool to advance into material. Such concept of physical model of keyhole laser welding was presented recently5) and a numerical code based on the "drilling" description of the keyhole front wall was proposed6).

The objective of this work was to study the weld pool behavior using high speed photography, and detection of acoustic and light emissions to develop further the concept presented earlier5), and to create a simple numerical code for simulation of keyhole front evolution.

2. Experimental Procedures and Results

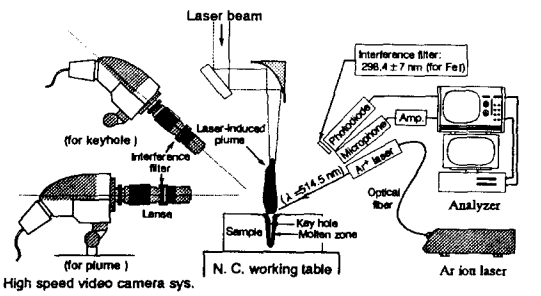

Fig.1 Schematic experimental setup for High speed video observation of plasma, keyhole, light emission and sound during CW CO2 laser irradiation

Fig.1 shows schematic experimental setup for observation of plasma, keyhole, light emission and sound during CW CO_2 laser was used to conduct welding experiment in the speed range from 25 mm/s to 300 mm/s. The beam-sample interaction zone was illuminated by an Argon-ion laser and was taken images of molten pool and laser induced plume/plasma by a Photron FASTCAM ultima video at the framing rate of 40,000 fps. A1/8 inch Bruer-Kjaer microphone

with flat response in the frequency range 4-100,000 Hz was placed at the 250mm distance from the beam-sample inter action zone.. Also a photo diode covered with 14nm bandwidth filter centered at 298.4 nm wavelength was used to detect the fluctuations of near surface plasma radiation intensity. The acoustic emission (AE) and light emission (LE) signals were recorded with a Yokogawa AR1200 oscilloscope, which allowed to store signals of several seconds length with 10 μs temporal resolution. A 10mm thick 304 stainless steel revealed that the melt flow at the front part of pool was changing periodically. It was also observed that the plume of evaporated material showed periodical variations of its intensity and direction which was synchronized with the melt flow fluctuations. At some moment the plume was perpendicular to the sample surface, plume intensity increased and a hump of the melt appeared at the leading edge of the weld pool in front of keyhole opening;. Then plume tilted in the direction of the sample moving and melt hump in the front part of the pool disappeared, but high amplitude melt wave occurred on the sides of the keyhole opening at the leading part of pool.. The plume at this time again became normal to the sample and its intensity decreased.

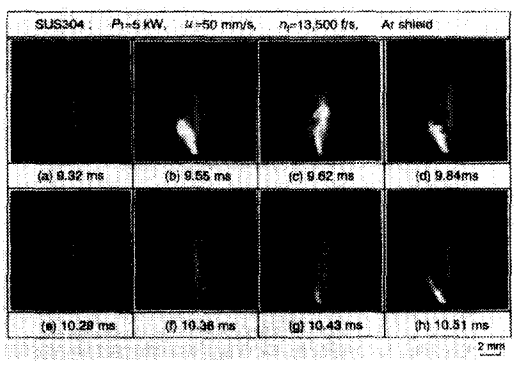

Fig. 2 High speed photographs of plasma /plume induced from SUS 304 during laser welding in Ar shielding gas.

Fig.2 shows high speed photographs of plasma/plume induced from SUS 304 during laser welding in Ar shielding gas.

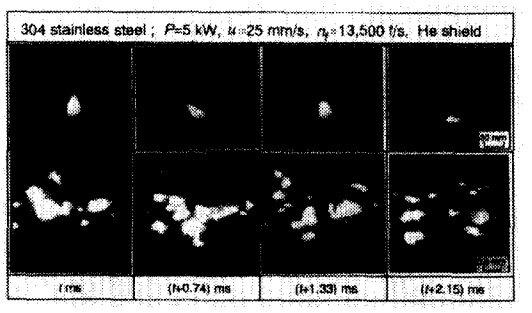

Fig. 3 Sequence of the periodical melt pool and plume

Fig.3 exhibits the sequence of the periodical melt pool and plume behaviors in case of laser welding of SUS 304 in He shielding.

The characteristic frequency of the cycle depended on the sample moving speed and type of shielding gas. It was found that the frequency stays in the ranges of 300-600 Hz, 450-600 Hz and 650-900 Hz for the moving speed of 25mm/s, 50mm/s and 100 mm/s, respectively. For further higher speeds it was difficult to determine the frequency values accurately, though estimation showed that they exceeded several kHz. When Argon was used as a shielding gas the melt evolution frequency during 304 steel welding was higher than for Helium case staying in the range above 1 kHz.

The existence and motion of a flake which was presumed to be slag was observed on the liquid surface in case of Ar and He shields as shown in Fig.4. The flake moved in the direction of the sample translation at the sides of the pool and in the opposite to the sample motion direction in the rear part of pool along the pool axis making vortices. The behavior of flake indicated that in the weld pool there existed a

high velocity turbulent flow which seemed to be originated from the beam impingement area and moving along the side walls of the pool. The flow reached the back wall, changed its direction to the opposite to sample moving direction and proceeded along the pool axis creating vortices.

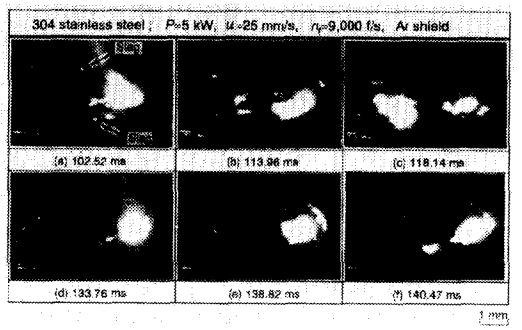

Fig. 4 Video frame representing slag motion pattern on the rear part of Weld pool

Fig.5 shows the spectra of acoustic emission (AE) and temporal fluctuations of plasma radiation intensity (LE) in different welding speed in He shielding. At the speed of 25 mm/s AE has the dominating frequencies ranging from 1 kHz to 4 kHz with a number not distinctive peaks at approximately 1.5 kHz and 2 kHz(Fig. 5(a)). Below 1kHz the amplitude of spectral components is relatively low and has distribution without dominating peaks(Fig. 5(b)). There is no evident correlation between AE and LE spectra at this low speed welding.

For the case of 100 mm/s moving speed, on the other hand, dominant peaks in the AE spectrum occur at approximately 800 Hz, 1.5 kHz, 2 kHz and 3.4 kHz(Fig 5 (c)). The corresponding LE spectrum contains low

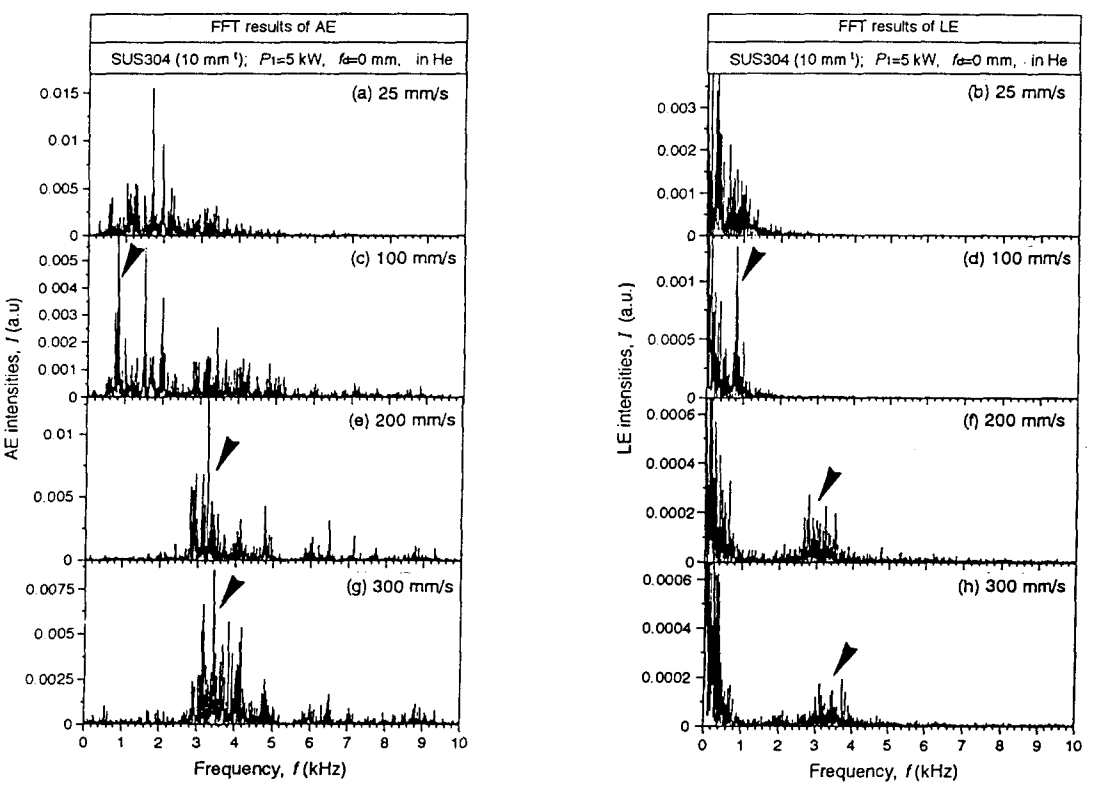

Fig. 5 spectra of acoustic (a,c,e,g) and light (b,d,f,h) emission fluctuation in different welding speed (P=5kW, He shield, 304 Stainless Steel)

frequencies in 0-500 Hz range and peak at 750-850 Hz(Fig. 5(d)). Thus, under this condition there is a correlation between the peaks in AE and LE spectra in the vicinity of 800 Hz. For higher translation speeds (Fig. 5(e, g)), AE contains high amplitude peak, which shifts to higher frequency area with increase of moving speed. Corresponding LE (Fig. 5(f, h)) have set of low frequency harmonics in 0-500 Hz range similarly to 100 mm/s moving speed case, and single peak also shifts to the higher frequencies with increase in translation speed coinciding with the AE spectra peak.

3. Physical Model of Keyhole Welding

The model is based on the following main assumptions; 1) Only front part of keyhole wall is exposed to the high intensity laser beam; 2) recoil pressure exceeds surface tension and hydrostatic pressures and propagation of keyhole inside the solid is due to the melt expulsion similarly to drilling; 3) flux of evaporated material is linearly proportional to the absorbed laser intensity minus heat losses; 4) recoil pressure resulting from laser induced surface vaporization equals to the product of the evaporated material flux and near surface vapor velocity; 5) thermal field is quasistationary. Unlike the latest work6), which supposed that the local keyhole "drilling" velocity was tangent to the keyhole, the present authors considered the keyhole wall propagation speed as normal to the keyhole wall. Also, for the sake of simplification, we assumed that the melt motion at the front part of keyhole was one dimensional with the direction toward the sides of the weld pool and that the laser beam intensity profile was Gaussian and uniform along the lines coinciding with and normal to the sample translation vector, respectively.

In work (5), the keyhole velocity was expressed through the power and radius of laser beam and thermophysical parameters of material (equation (9)). In this equation variable P denotes the part of absorbed laser beam power left after part was spent to bring the surface temperature up to vaporization temperature and induce vaporization. Modification of equation (9) from work (5) gives more convenient equation relating the local wall velocity νd to the local absorbed intensity of laser beam $I abs$ in the following form:

$$\nu d=\sqrt{\frac{\alpha}{\gamma L}\frac{\rho m}{\rho s}\sqrt{\frac{2}{\rho m}\left|\left(Iabs-\frac{K}{\alpha}(Tv-Tm)u\right)\frac{\nu T}{Lv}-\frac{\sigma}{\gamma L}\right|}} \quad \cdots\cdots(1)$$

where, ρm and ρs are the density of liquid and solid, υ is sample (or beam) translation speed, νT is vapor velocity in the Knudsen layer, κ and α is heat conductivity and diffusivity correspondingly, Lv is latent heat of vaporization, σ is surface tension and γL is laser beam radius. The second term in the round parenthesis represents the losses for the heat conduction assuming the gradient of temperature equal to the ratio of the difference between vaporization and melting temperatures and heat penetration depth for moving source equal to α/υ. The second term in the square parenthesis appears when the requirement that recoil pressure must exceed the surface tension pressure is introduced.

The local absorbed laser intensity $I abs$ can be expressed through incident beam intensity at the material surface $I incs$ as follows.

$$I_{abs} = I_{inc}{}^{s}A(\alpha)\cos\alpha \quad \cdots\cdots(2)$$

where, α is the angle between the laser beam

axis and the local normal to the keyhole wall surface, A is angle dependent coefficient of absorption which in the calculations was assumed as the following function $Ao\ \cos 0.2(\alpha)$ with Ao as a normal incidence absorption coefficient.

If the absorption in the keyhole plasma is taken into account and the refraction is disregarded, the laser intensity at the keyhole surface can be expressed through the laser beam intensity I_L as

$$I_{inc}^{s} = I_L \exp\left(-\int_0^{lp} \mu(l)dl\right) \quad \cdots\cdots\cdots (3)$$

where, lp is the local length which a ray must travel in the plasma to reach the keyhole surface, $\mu(l)$ is the distribution of plasma absorption coefficient which is determined by the gas dynamics and ionization kinetics of the vapor jet and shield gas.

Thus, if the absorption coefficient distribution in plasma is known or calculated, the instantaneous drilling velocity at a certain time can be expressed through the laser beam intensity and thermophysical parameters of the material and equation (1) describes the dynamics of the propagation of the front part of keyhole into material.

4. Numerical Simulation Results

Unlike the existing models which assumed that the velocity of keyhole propagation into material is parallel to the beam translation vector and equal to the beam moving seed, our calculations show that this velocity can be directed under some angle relative to the sample velocity vector and the absolute value of the component parallel to the sample translation vector (x-component in this paper) can be lower, equal or higher than the sample moving speed, depending on the welding conditions. The calculated profile of the x-component of keyhole wall propagation velocity indicates that some parts of the wall move from the beam axis, while other move toward axis. The reason for the generation of such wall velocity distribution is as follows. If for the given conditions the keyhole wall propagation velocity has negative x-component, the keyhole wall moves from the laser beam axis into the area of lower laser intensity and reaches the zone where laser intensity is lower than the threshold value required to zero and the x-component of the wall velocity becomes positive with the value equal to the sample translation speed. The keyhole motion toward the beam axis continues until the higher laser beam intensity area is reached, then the vaporization is established and melt ejection takes place again. The keyhole wall reaches the threshold position in different moments at different keyhole locations, and some parts of the keyhole move from the beam axis while other parts move toward the beam axis, Thus, humps are formed on the front part of keyhole wall. The simulation results show that the bumps originated at the top part of keyhole move down the wall and disappear at the bottom. The amplitude of the humps is much smaller than beam or keyhole radius. Since this instability occurs because the keyhole wall moves faster than the laser beam translation speed, the humping of the front part of keyhole wall can be called "runaway" instability.

With the increase of the sample moving speed the spatial frequency of the humps increases and their amplitude decreases until x-component of keyhole velocity becomes smaller than the beam

translation speed. After this threshold speed reached the hump formation does not occur and a quasistationary state of keyhole propagation into material is achieved. According to the preliminary results of calculations for the case of Gaussian beam intensity distribution the threshold velocity of "runaway" instability existence is either independent or depends weakly on thee laser beam intensity, butt strongly decreased with the laser beam radius increase. Calculations show that for the typical welding condition of steel the threshold translation speed is in the range of 200-400 mm/s (12-24m/min). Since the model incorporates significant simplification these result requires additional verification of beam intensity and distribution dependencies using more advanced ode. Also the numerically predicted value of threshold velocity might be closer to thee experimentally observed range of 100-200 mm/s when more detailed code is used.

Experimental data obtained inn the case of EB welding indicate that thee number of humps on the keyhole front wall is small(several humps)..

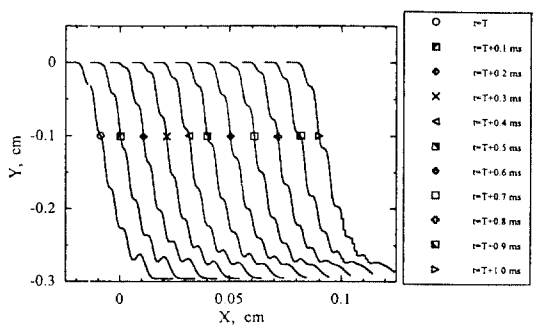

Fig. 6 Evolution of keyhole front wall when melt inertia is tsken into account. (P=3kW, rL=140㎛, u=100 mm/s)

If the melt inertia, determined as the time required to establish melt flow, is included in the code it predicts the lower number of humps(5 or 6 humps) and higher hump amplitude(1/5 or 1/4 of keyhole opening radius). The results of "runaway" simulation show the hump formation and its propagation along the wall as shown in Fig. 6. The characteristic time for the generation of the humps at the keyhole opening is about 1ms for the case of steel welding with 3kw CO2 laser focused down to a spot off 140 μm radius with Gaussian intensity distribution.

Besides the prediction of the "runaway" instability the present numerical model shows that the melt ejection velocity can reach 1 m/s. Consequently, in the calculations of thermal field in the weld pool the convective heat transfer must be considered in addition to the conductive mode of heat propagation. Also high speed melt flow originated in the front part of keyhole seems to play important role in generation of pool volumetric oscillation, spattering fromm the weld pool and other defects formation.

5. Discussion

The comparison of the simulation results, which predict "runaway" instability of front part keyhole wall and generation of high speed unstable melt flow from the beam impingement area, and the experimental observations shows that predictions of the model are qualitatively consistent with the experimentally obtained results. En the basis of combined numerical and experimental results the following description of the pool dynamics and interpretation of AE and LE spectra fluctuation con be proposed

According to the numerical results the hump formation at the top part of the keyhole starts with initiation of the vaporization of melt surface

which previously run away from and then moved into the higher intensity area of the incident beam. The melt surface moved into the beam at the top is practically normal to the laser beam, thus, the plume of the evaporated material must be normal to sample surface. After the delay determined by the melt inertia time the ejection of liquid metal from the hump area occurs and the hump propagates down the keyhole. This must be accompanied with the vapor plume tilt toward the direction of sample translation and formation of the melt waves on the sides of the pool close to the keyhole opening. When the hump reaches deeper level in the keyhole and the keyhole wall at the top moves away from the beam the plume becomes less brighter and regains direction perpendicular to the sample surface and waves on the sides of the pool decrease in amplitude. Thus the moment when on the high speed video the plume becomes brighter having perpendicular to the sample surface direction, probably, corresponds to the moment of the beginning of the hump formation at the top of keyhole wall. Approximately 300-500 μs after that a crown like melt wave occurs on the front and side parts of the pool in the keyhole area and plume tilts in the sample translation direction. Then the plume regains normal to the sample direction with decrease in brightness, the wave on the pool sides moves further into the pool and the amplitude of melt crown on the front and side parts of the keyhole area decreases. this cycle repeats after each 1-3 ms depending on the sample moving speed.

Near surface plasma brightness variations must be influenced by the dynamics of keyhole opening and consequent change of the vapor plume direction. Thus, the low frequency part of the plasma LE fluctuation with peaks positioned at the hump formation frequency and shifting from 300 hz to 4 kHz with sample moving speed from 25 mm/s to 300 mm/s corresponds to the keyhole "runaway" instability. Since these low frequency peaks have relatively higher amplitude one can conclude that the keyhole instability is the primary factor determining the plume brightness fluctuations.

The AE spectra recorded at low sample travel speed have small amplitude low frequency peak coinciding with plasma brightness fluctuation (hump formation) frequency, and the high amplitude high frequency(2-4 kHz) peaks which vanish with sample speed increase.. Increase of the translation speed results in more pronounced low frequency AE peak, probably because harmonics in the 2-4 kHz range disappear. When sample travel speed becomes faster this peak shifts to higher frequency region similarly to the LE spectra. The AE amplitude in 2-4 kHz region goes down to zero when the moving speed becomes such that the penetration depth decreases to value smaller than weld width, and the formation of well developed keyhole does not occur. It allows to suggest that the high frequency components of the AE signal originate from the interaction of the vapor jet with the keyhole surface. Since the amplitude of these harmonics is comparatively high, the vapor-wall interaction is the dominating factor for the sound generation.

6. conclusions

The major conclusions obtained in this work are as follows:

1) High speed video photography of laser welding showed the existence of fluctuating high speed melt flow which seems to be originated from the laser beam impingement

area creating the side waves at the front part of weld pool, then flowing along the side wall of keyhole, turning at the rear part of weld pool and proceeding in the opposite direction along the pool axis creating rear part of weld pool and proceeding in the opposite direction along the pool axis creating vortices. This melt flow cannot be ignored if the adequate numerical simulation of thermal field and hydrodynamic stability of the pool are of concern.

2) The low frequencies dominating in fluctuation spectra of plasma light emission (LE) probably reflect keyhole opening instability. These low frequency peaks shift to higher frequency area with the welding speed increase. Acoustic emission (AE) spectra contain relatively small amplitude low frequency part and dominating high frequency peaks which, probably, originate due to vapor jet interaction with keyhole wall. High frequency AE harmonics disappear with transition from keyhole to shallow penetration welding, while low frequency AE spectra peaks shifts to higher frequency area similarly to the LE spectra behavior. Thus experimental data together with simulation results are consistent with assumption that in the keyhole welding LE fluctuation spectra carry information on the keyhole opening dynamics, and AE spectra reflect keyhole front wall behavior and vapor jet-keyhole wall interaction.

3) The numerical model, based on the approach which considers the keyhole propagation into material at high welding speed ass an essentially drilling process, predicts formation of the humps on the front part of keyhole wall ("runaway instability"). The predicted hump formation frequency and its dynamics are consistent with observed melt dynamics.

4) Developed keyhole model indicates the existence of high velocity melt flow as high as 1 m/s, which is capable of influencing heat transfer dynamics and weld pool hydrodynamic instability.

references

1) Y. Arata : plasma, Electron and Laser Beam Technology-Development and Use in Material processing-, ASM International, (1986), pp. 641-650.

2) J. D. Kim, S, Katayama and A. Matsunawa : "Formation Mechanism and Prevention of Defects in Laser Welding (Report 1)-Effects of Pulse Shapes on Keyhole Behavior-", Preprints of the National Meeting of Japan Welding Society, Vol. 59(1996), pp. 74-75.

3) J. D. Kim, S, Katayama and A. Matsunawa : "plasma Diagnostics in Pulse YAG laser Welding", The 6th International Symposium on the Role of Welding Science and Technology in the 21st century, Nagoya Japan, Nov. 19-221, Vol.1(1996), pp. 203-208.

4) S. Katayama, J. D. Kim and A. Matsunawa : "YAG laser welding phenomenon", Proceeding of 40th Laser Materials Processing conference, Osaka Japan, March 13-14, (1997), pp. 21-31.

5) V. V. Semak, J. A. Hopkins, M. H. McCay : "A Concept for a Hydrodynamic Model of Keyhole Formation and Support during Laser Welding", Proc. ICALEO'94, (1994) pp. 641-650.

6) R. Fabbro & A. Poueyo-verwaerde : "Modeling of Deep Penetration Laser Welding Process - Application to the Analysis of the Energy Coupling inside the Keyhole - ", Proc. ICALEO'95, (1995), pp. 979-988.